

Air curtain temperature measurement in an open refrigerated display cabinet by IR thermography

by S. Marinetti*, A. Rossetti*, F. Ferrari* and S. Minetto*

* National Research Council, Construction Technologies Institute, Corso Stati Uniti, 4, 35127 Padova, Italy, email: sergio.marinetti@itc.cnr.it

Abstract

IR Thermography has been widely used to measure air temperature in many application fields. Usually screens or targets are located in the region of interest in such a way to minimize the perturbation of the flow under investigation. In this work, this technique is applied to map the air distribution inside the cold curtain of an open refrigerated display cabinet (ORDC). The performances of the commonly used black cardboard and a net-screen are studied in different conditions by a CFD analysis. Experimental measurements are carried out on the cold curtain, both with the cardboard and the net-screen. The comparison of results is reported.

1 Introduction

Air temperature measurement by IR thermography is a well known topic, and many works can be found in literature. We can consider two main applications: local measurements, oriented to obtain quantitative information, and temperature distribution mapping, aimed at achieving qualitative information.

In [1], the local air temperature was measured by means of an aluminium case, which was supposed to be in thermal equilibrium with the air. The target had a low emissivity frame, and a central cavity. The reflector allowed accounting and compensating for the overall reflected IR radiation coming from the surroundings. The central cavity, observed by the IR camera, worked as a black body providing the air temperature. A similar approach was used in [2], for indoor local air temperature measurements in a laboratory, in a garage, and in a subterranean structure. The discrepancy between IR thermography and temperature probes was less than 0.4°C. In these cases, the attention was mainly drawn to the measurement accuracy to the detriment of the spatial resolution, due to the target encumbrance. Indeed, to this purpose, the target has to provide local detailed information about the reflected and emitted IR radiation, thus requiring for each measurement point both a reflective and high emissive reference.

Instead, mapping the air temperature distribution requires high spatial resolution data, therefore uniform screen are usually used. In [3], a scenery paper was used to qualitatively analyse the temperature distribution produced by a commercial air curtain device. A numerical parametric study, based on different variables like door height, temperature difference between two compartments, initial angle and velocity of the jet, was carried out and experimental data showed a good agreement with the expected behaviour. In [4], a black cardboard was used in an ORDC to validate the temperature field predicted by a CFD model. The infrared temperature readings were calibrated by nine thermocouples located on the surface of the flat plate with emissivity of 0.96. The field data comparison showed a good "global" agreement, i.e., the authors demonstrate that the air curtain was fairly effective in maintaining the temperature inside the display case over an acceptable range. In [5], air temperature was measured with an infrared camera and a measuring screen placed in the airflow, close to a low-velocity diffuser in displacement ventilation. The purpose of this study was to conduct a parameter and error analysis of the proposed whole-field measuring method. A model of the energy balance, for a solid measuring screen, was used for analyzing the influence of different parameters on the accuracy of the method. Assuming negligible the effects of the lateral heat conduction, the authors considered the effects of the radiation and suggested, as a compromise to reduce the measurements errors, the use of a two-material screen with high emissivity on the surface facing the IR camera and low emissivity on the other side (for instance using paper and a glossy aluminium layer). In such a way, while the effect of the surrounding radiation is reduced, the in-plane thermal conductivity is increased thus causing the deformation of the temperature distribution.

Summing up, the choice of the screen is a crucial point to obtain reliable results. A good screen should be the best compromise between the following main requirements:

1. heat conduction between the measurement points on the screen surface (that is the in-plane thermal conductivity) must be low to ensure a good spatial resolution;
2. radiative heat flux must be negligible in order to account only for the convective heat exchange, thus requiring a low emissivity value;
3. emissivity must be high to reduce the amount of reflected radiation hitting the IR detector so that minimizing the measurement error.

In this work, the use of a plastic net with aluminium targets is proposed. One side of the target was blackened to meet point 3, and the other was left reflective to meet point 2. The use of a net with thin plastic wires allowed fulfilling

point 1. The actual emissivity value of the paint use to blacken the targets has been previously assessed according to the procedure described in [6], in order to enhance the measurement accuracy.

A numerical CFD analysis was carried out considering the single and combined contributions of the involved parameters, in order to assess the expected performance of the proposed solution.

2 Experimental results

Experimental tests were carried out on an ORDC, locating the screens in the symmetry plane of the cabinet at the lower part of the cold curtain as showed in Fig. 1a.

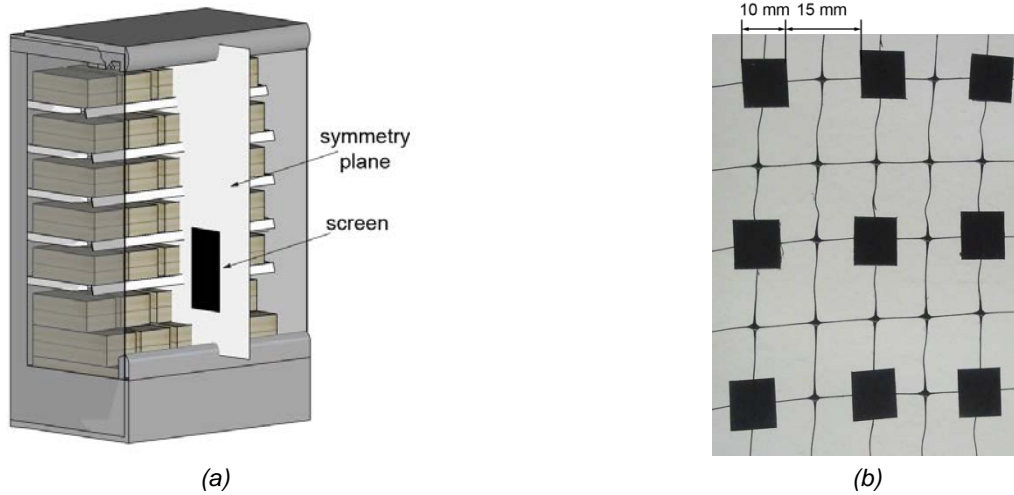


Fig. 1. Sketch of the experimental test (a); net with aluminium targets (b).

Two kinds of screens were used: traditional black cardboard and aluminium targets with one blackened face and the other left reflective (Fig. 1b). Sequences of 60 IR images were recorded by a FLIR SC6000 HS MW camera at a sampling interval of 1 s. The observation time and the sampling rate were chosen based on a previous analysis to reliably detect the average temperature field.

In comparison to the target grid (Fig. 2b), the cardboard (Fig. 2a) exhibits a smoother pattern and a higher mean temperature. The two temperature maps differ up to 3°C (Fig. 2c).

These discrepancies can be ascribed to the different way in which conduction, convection and thermal radiation modify the screen equilibrium temperature.

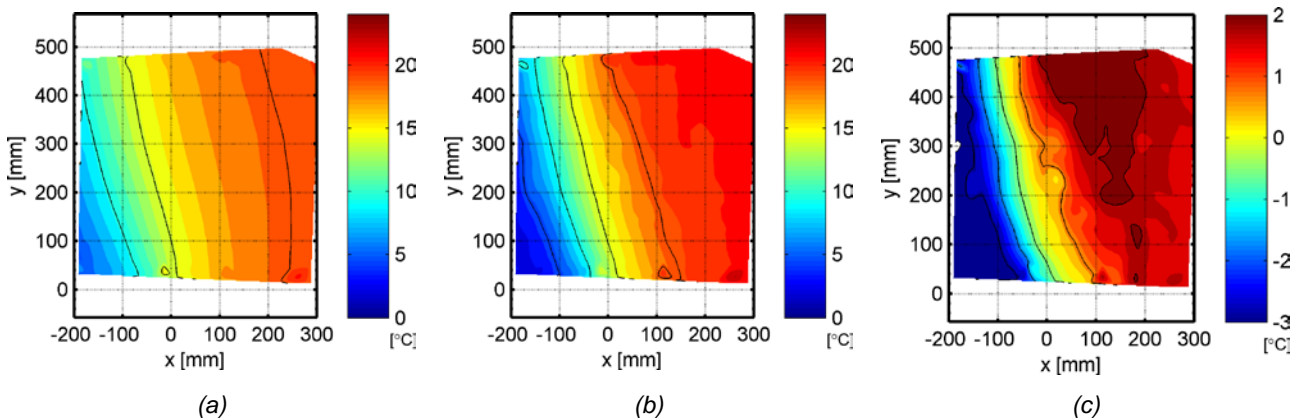


Fig. 2. Experimental temperature maps: cardboard (a), target grid (b), difference (c).

The question was whether the proposed target screen, which is thought to get a good compromise between the three requirements listed in section 1, is actually better than the traditional cardboard and, in the case, what is the adherence of the measured temperature field with respect to the corresponding undisturbed area.

CFD models were then employed to quantitatively evaluate the measurement accuracy and the contribution of each error source.

3 CFD analysis

Numerical analysis was conducted to assess the systematic measurement errors when using the black cardboard and the target net. Commercial software COMSOL MULTIPHYSICS 4.4 was used for all the models.

Despite the case study allows a 2D description (at least on the symmetry plane of the ORDC), the presence of the screen cannot be accounted without a full 3D model, due to the presence of the boundary layer development on the screen surface.

In order to get realistic boundary conditions for the 3D model of the air flow around the screens, a 2D model of the whole curtain was developed. The following paragraph will first present this model and its results, detailing subsequently the set up of the 3D models.

3.1 ORDC 2D model

The free flow of the air curtain was first solved in a 2D model representing the symmetry plane of the ORDC, assuming the effects of the finite extensions of the cabinet to be negligible in this section. The main boundary conditions and the model sketch are reported in Fig. 3 and Table 1. The opening condition was set to simulate the interaction of the model with an infinite plenum at constant temperature and constant total pressure. Ambient references were set to 25 °C for the temperature and 1 atm for the pressure. The ambient pressure was used as total pressure when the flow was entering the model; on the contrary it was assumed to be a static pressure boundary when the flow was exiting the model. Similarly, the temperature was used as a boundary for the entering flow, while a temperature outflow condition was set where the flow was leaving the numerical domain. Average velocity at RAG was set to exactly balance the mass flow entering the domain from the RAG and the BP.

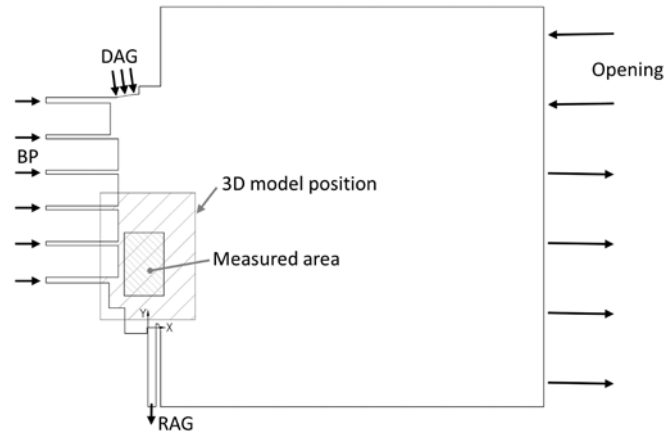


Fig. 3. Sketch of the ORDC 2D model with boundary and coordinate system.

Table 1. ORDC 2d model boundary condition

Location	Boundary	Value
DAG (Discharge Air Grille)	Velocity - Temperature	0.7 [m/s] - 0.5 [°C]
BP (Back Panel)	Velocity - Temperature	0.3 [m/s] - 0.5 [°C]
RAG (Return Air Grille)	Velocity	2.32 [m/s]
Opening	Opening Pressure-Opening Temperature	1 [atm] - 25 [°C]

Dry air ideal gas was used as fluid. The effect of buoyancy was accounted into the domain. Air turbulence was modelled using the k-epsilon turbulence model and the flow-wall interaction was accounted using wall functions.

Results are reported in Fig. 4, where velocity and temperature are shown.

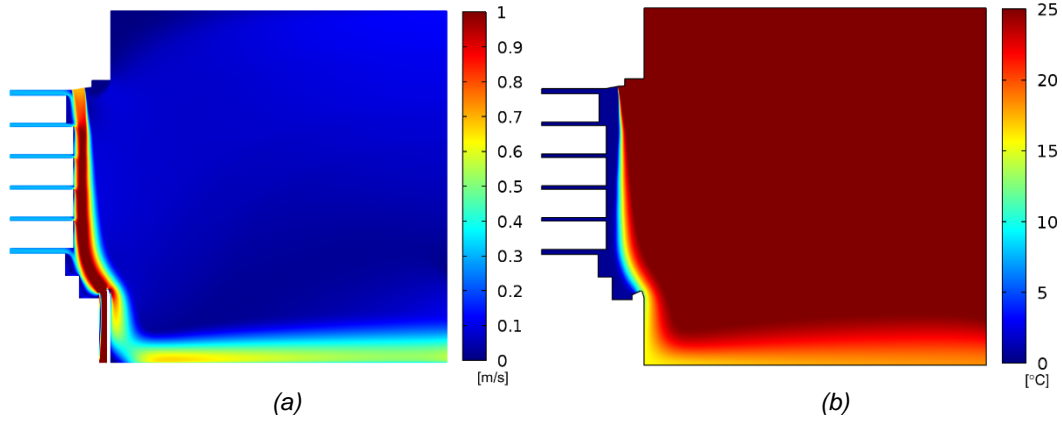


Fig. 4. ORDC 2D model results; a) velocity [m/s]; b) temperature [°C].

3.2 Numerical model of the screens

As mentioned above, the presence of the screen in the ORDC air curtain cannot be accounted without a full 3D model, due to the presence of the boundary layer development on the screen surface. The 3D CFD domain was defined as a hexahedron volume 0.8 m high, 0.6 m wide and 0.25 m deep, enclosing the lower part of the curtain. The measured area (i.e. the screen) was placed on a side of this volume, assuming the system to be symmetrical with respect to the measuring plane. Domain geometry is reported in Fig. 5.

Boundary values were extracted from the 2D model. Velocity, temperature and turbulent quantities were set on the sides of the model, except for the lower surface where static pressure was set. Thermal radiation was considered in order to account for the effect of the surrounding environment. As the model did not enclose all the radiating surfaces, the view factors were computed analytically, assuming the radiating elements to be perfect black bodies. The adopted model is sketched in Fig. 5c, which reports the top view of the fluid domain and the ORDC profile. Let $T_g = 5^\circ\text{C}$ be the temperatures of the exposed goods, $T_s = 15^\circ\text{C}$ the ORDC side-wall temperature, and $T_a = 25^\circ\text{C}$ the ambient temperature, radiation to point p was computed as:

$$q_{rad}(p) = \epsilon \sigma (T^4 - T_{eq}^4) \quad (1)$$

where

$$T_{eq}^4 = \frac{\cos\theta_g}{2} T_g^4 + \frac{2 - \cos\theta_g - \cos\theta_a}{2} T_s^4 + \frac{\cos\theta_a}{2} T_a^4 \quad (2)$$

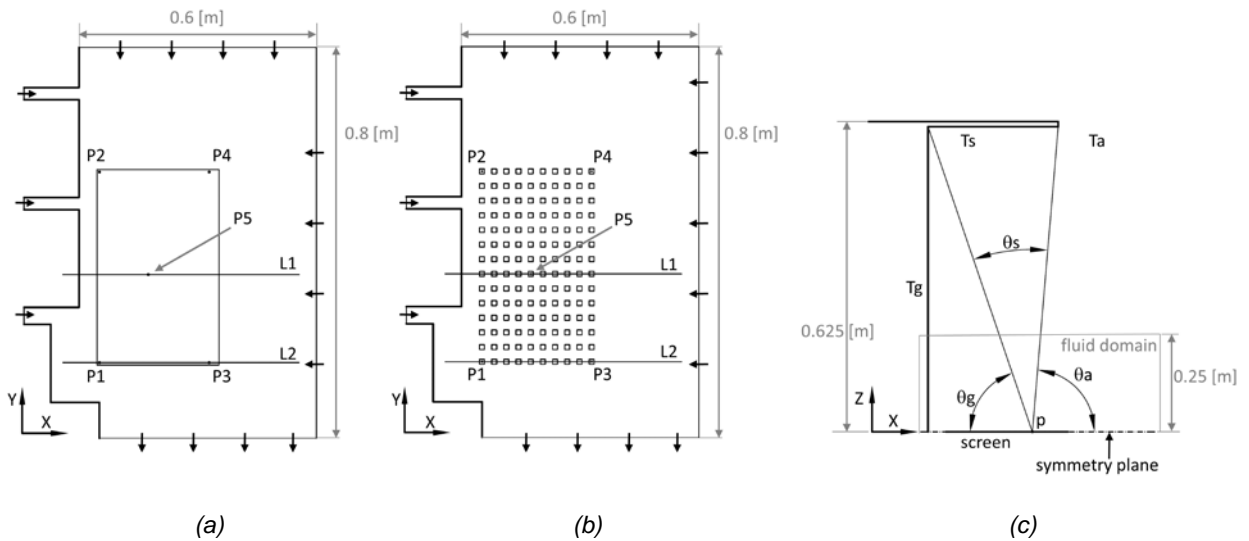


Fig. 5. Numerical model geometry and boundary; a) cardboard screen; b) net screen; c) sketch of the geometry used for the view factor calculation.

Tetrahedral grids were employed for the discretisation. Prism layer were used to improve accuracy close to walls, both on the screen and on the ORDC profiles. Grid sensitivity was carried out in order to define a good grid independent solution. Results are reported in Fig. 6a, where the temperature of the five points shown in Fig. 5a, are plotted as a function of the node number on the cardboard surface. As a result of the study, the grid characterised by 70000 nodes on the cardboard was assumed as the best compromise between accuracy and computational effort.

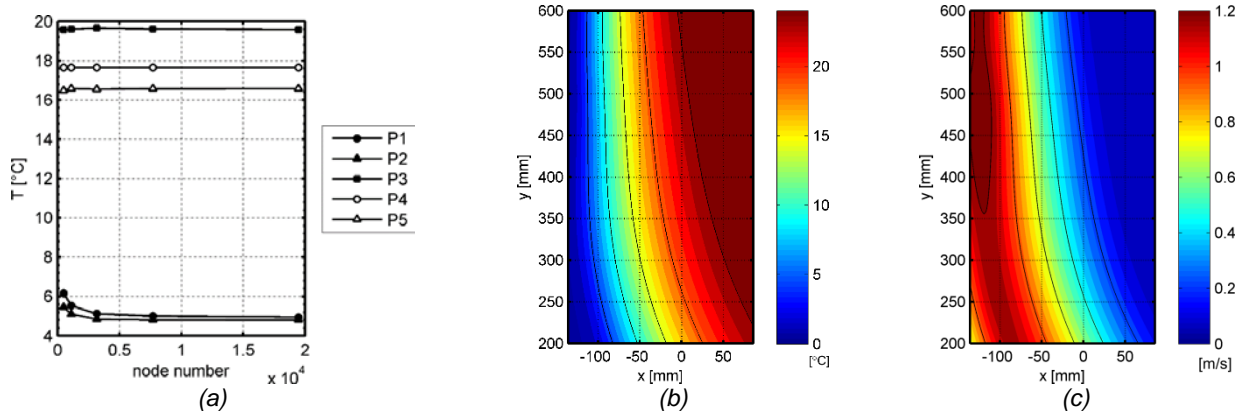


Fig. 6. Results of the sensitivity study (a); undisturbed temperature distribution on the symmetry plane (b) and the corresponding velocity field (c).

Fig. 6b and Fig. 6c depict the undisturbed temperature and velocity distributions, provided by the 3D CFD model, on the symmetry plane, corresponding to the area covered by the screen. As it can be seen from the figure, this area is subjected to important temperature and velocity gradient. In the following discussion, this temperature map is considered as the reference to assess the discrepancies caused by each measurement disturbance.

4 Numerical Results

4.1 Effect of the presence of the screen in the air flow

Placing the screen in the air flow is an intrusive action that has the effect of locally changing the velocity field and consequently the heat transfer. In this analysis we neglect the surrounding thermal radiation and the screen in-plane conductivity, thus taking into account only the convective heat exchange between the air flow and the screen. To this purpose, two screens were considered: an ideal homogeneous sheet with a very low in-plane thermal conductivity ($k = 10^{-6} \text{ W m}^{-1} \text{ K}^{-1}$), and the target net of Fig. 1b. In addition, a third case was analysed to evaluate the effect of the actual thermal conductivity of the cardboard ($k = 10^{-1} \text{ W m}^{-1} \text{ K}^{-1}$).

The comparison between the surface temperature on the screens and the reference are shown in Fig. 7.

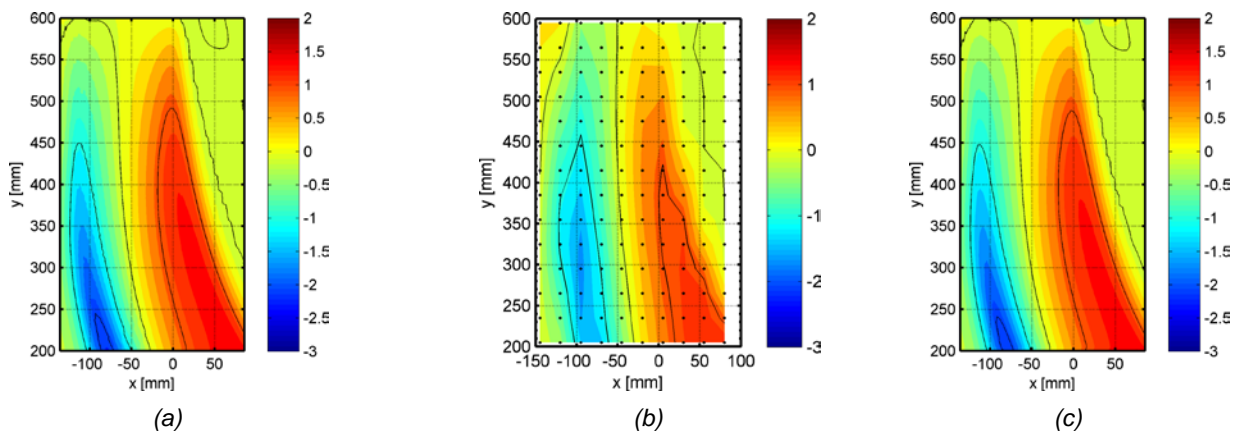


Fig. 7. Difference between the temperature map on the screen and the reference: homogeneous sheet with low in-plane conductivity (a); target net (b); cardboard screen (c).

As far as the temperature values are concerned, it can be noticed that, even using an ideal screen, leads to a temperature differences up to 3°C with respect to the reference (Fig. 7a). Comparing Fig. 7a and 8c, it seems that, for this application, the in-plane conductivity of the cardboard has no effect on the temperature distribution.

The patterns exhibited by all the images are very similar, with and underestimation inside the air curtain and an overestimation outside the curtain. Hence, based on surface screen temperature, the air curtain appears colder and the transition between cold and warm room air sharper. This is coherent with the presence of the boundary layer on the screen surface, which, dumping the free stream turbulence, reduces the mixing process between the curtain and the ambient. The temperature map on the screen could be therefore misleading in assessing the insulating properties of the curtain and the warm air infiltration from the ambient. Indeed, Fig. 8 shows how at $y=600$ mm, where the screen effect is still negligible, the curtain on the screen have the same width as in the undisturbed area, while at $y=300$ mm the curtain appears narrower than it is.

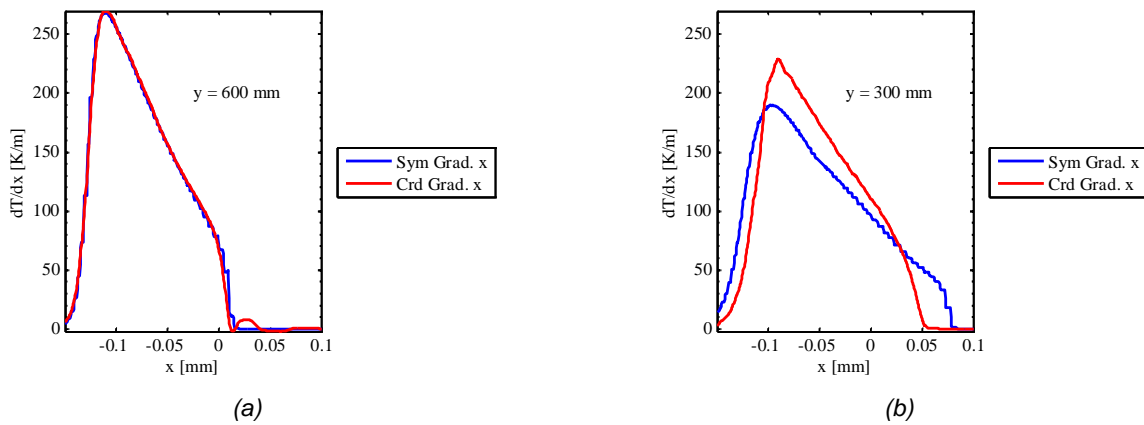


Fig. 8. Profiles of the temperature gradient along the x axis at $y=600$ mm (a) and $y=300$ mm (b).

Looking at the patterns in Fig. 7 and the profiles in Fig. 8, it can be noticed that the discrepancies grow from the top to the bottom of the screen, according to the main stream, which goes from the DAG to the RAG (Fig. 3). To better understand whether this fact can be imputed to a cumulative effect linked to the boundary layer growth, further numerical simulations have been carried out, considering, instead of the whole screen, a 10 mm high cardboard stripe and a single line of targets located in positions L1 and L2 (Fig. 5a). The differences between the temperature profiles taken on the whole screen and on the single line, with respect to the reference, are shown in Fig. 9a (cardboard) and Fig. 9b (targets). As expected, in both cases, the stripe (dotted lines) is less intrusive, and its temperature is closer to the reference one. However, it can be noticed that, in the region with the highest air speed (-150 mm $<x<-50$ mm), the cardboard in L2 shows a greater error than in L1. This behaviour is in line with the proposed explanation

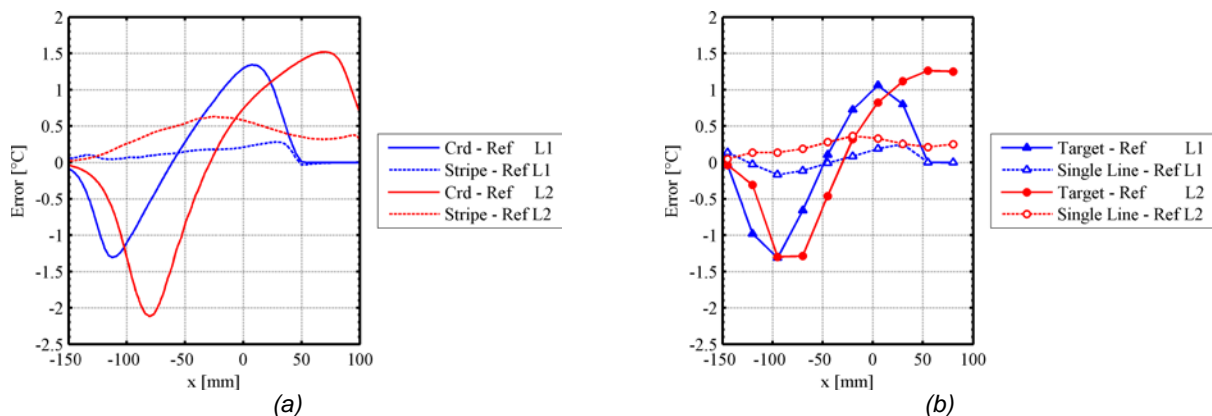


Fig. 9. Temperature difference, along L1 and L2, between the reference (Ref), the whole screen and the stripe/single line: cardboard (a); targets (b).

4.2 Effect of surrounding radiation

The radiative heat exchange between the screen and the surroundings (exposed goods, ORDC side-walls, and the room) has been added to the numerical analysis described in the previous section. This contribution, depending on factors that are external to the air curtain, interacts unexpectedly with the fluid-dynamic disturbance and therefore general comments cannot be easily made. In our case, since all the sources are warmer than the air inside the ORDC, the curtain temperature is overestimated by about 5°C with the cardboard, which is high emissive on both sides. The advantage of using targets with one reflective surface, thus reducing the radiation effect without compromising the overall in-plane conductivity, appears clear by observing Fig. 10. The pattern exhibited in Fig. 7 is overridden by the effects of the radiative heat transfer, and the discrepancies are larger.

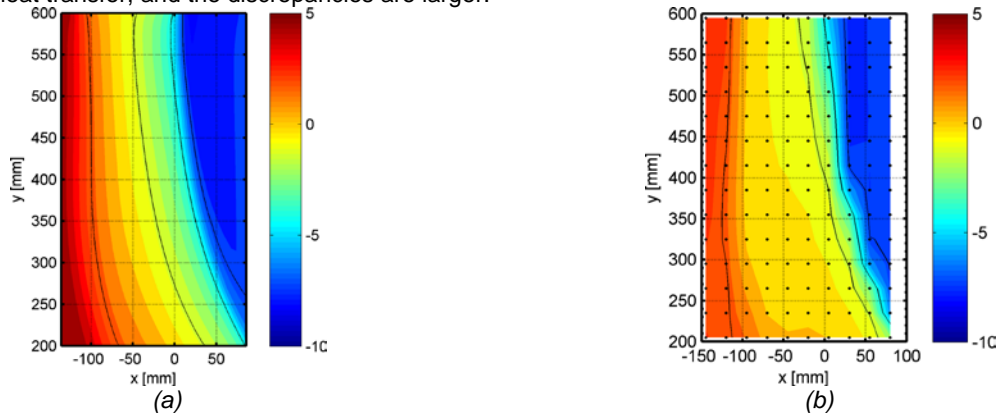


Fig. 10. Difference between the temperature map on the screen and the reference taking into account the radiative heat exchange: cardboard (a); targets (b).

Fig. 11 shows the temperature error profiles along L1 and L2 for both the whole screen and the stripe/single line. Now the benefit of the stripe is no longer so evident as in Fig. 9, thus confirming that in this case the radiative heat transfer plays an important role, whose effects are dominant over the velocity field perturbation caused by the whole screen.

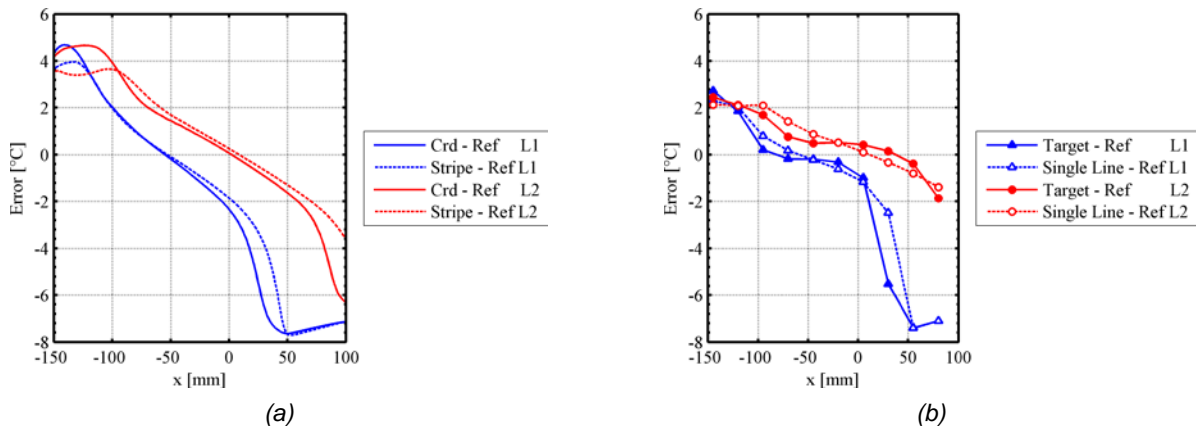


Fig. 11. Temperature difference, along L1 and L2, between the reference (Ref), the whole screen and the stripe/single line: cardboard (a); targets (b).

5 Conclusions

Thermographic technique was applied to measure the air temperature of the cold curtain in an ORDC. Two kinds of screens, a commonly used black cardboard and a net with aluminium targets, have been used. Through a CFD model of the air curtain portion containing the screen, an analysis of the fluid dynamic disturbance and the radiative heat transfer process was performed.

The presence of a screen influences the air mixing in proximity of its surface, and therefore the temperature distribution detected by the IR camera differs from that of the undisturbed flow, causing an apparent distortion of the curtain thickness. This must be taken into account when making considerations about the insulating performance of the curtain and its interaction with the ambient warm air. In our case study, the temperature error due to the air velocity disturbance is less than 2°C.

Considering the radiative heat exchange between the screen and the surroundings, the temperature error rises to 5°C inside the curtain and up to 8°C on the room side.

General conclusions about the magnitude of the fluid-dynamic and the radiative contributions cannot be drawn, but some considerations can be made. The thermal conductivity of the cardboard seems to be adequate for this kind of application. Indeed, numerical model of very low conductive screen does not show an improvement of the spatial resolution of the temperature field. From this point of view, the cardboard has the same performance as the target net. On the other hand, aluminium targets cause a slightly smaller perturbation of the velocity field. Better results could be obtained by using a cardboard stripe or a single target line. The screen temperature is influenced by the radiative heat exchange with the environment, as well. This contribution, which depends on the experimental layout and the surroundings, caused the temperature error to be raised. Using aluminium targets with one surface left reflective gives better results than the cardboard which is high emissive on both sides.

Finally, measuring air temperature by observing through an IR camera a screen immersed in a flow is an intrusive technique whose reliability and accuracy must be carefully assessed for each case.

REFERENCES

- [1] P.G. Bison, G. Cortelazzo, E. Grinzato, P. Svaizer, "Automatic thermal reference detection in thermographic images", SPIE Thermosense XII Proc., Vol. 1313, pp. 269-277, 1990.
- [2] C. Porrás-Amores, F.R. Mazarrón, I. Cañas, "Using quantitative infrared thermography to determine indoor air temperature", Energy and Buildings, Vol. 65, pp. 292-298, 2013.
- [3] Neto L.P.C., Gameiro Silva M.C., Costa J., "On the use of infrared thermography in studies with air curtain devices", Energy and Buildings, Vol. 38, pp. 1194-1199, 2006.
- [4] Navaz, H.K., Faramarzi, R., Dabiri, D., Gharib, M., and Modarress, D., "The Application of Advanced Methods in Analyzing the Performance of the Air Curtain in a Refrigerated Display Case," Journal of Fluid Engineering, ASME Transactions, Vol. 124, pp. 756-764, September 2002.
- [5] M. Cehlin M., Moshfegh B., Sandberg M., "Measurements of air temperatures close to a low-velocity diffuser in displacement ventilation using an infrared camera", Energy and Buildings, Vol. 34, pp. 687-698, 2002.
- [6] Marinetti S., Cesaratto P.G., "Emissivity estimation for accurate quantitative thermography", NDT&EInternational, Vol. 51, pp. 127-134, 2012.